A Brief Introduction to Scanning Electron Microscopy

Daniel Korchinski, Johannes Duereth, Robyn McNeil, Mia Au, Valentin Schmid
(Dated: November 19, 2019)

Scanning Electron Microscopy (SEM) is a technique for image generation that, owing to its operational simplicity, short imaging time, and nanoscale spatial resolution, is now prevalent in many fields of industry and research. Here, we review the key theoretical and experimental underpinnings of SEM, including pertinent details regarding data processing, image acquisition, and other experimental considerations. We also highlight recent developments in thin film studies, fractography, and nanomaterials as example applications of SEM in modern research.

I. INTRODUCTION

When speaking at a nanotechnology conference in late '59, Richard Feynman is reported to have said, "it is very easy to answer many of these fundamental biological questions; you just look at the thing!" [1]. The first commercial scanning electron microscope, sold in '65, aimed to realize that statement. Traditional optical microscopes, have a resolution d limited by Abbe's equation,

$$d = \frac{0.612\lambda}{n\sin(\alpha)}\,, \tag{1}$$

where d is the minimum resolvable distance, the 0.612 comes from the radius of the Airy disk (cf. Supplementary Figure 11), λ is the associated wavelength, n is the optical system's index of refraction, and α is half the aperture angle. The best case is $n\sin\alpha \approx 1$, which for green light (500 nm) yields a maximum resolution of ~ 300 nm. To go beyond this limit, shorter wavelengths are required. By using accelerated electrons, wavelengths down to 25 pm can be probed, with de Broglie's relation. This motivates the use of electrons as a probe for short-scale physics, but only if one has a way to "see" using electrons. The principle is relatively straightforward, and has not changed much since M. von Ardenne's first SEM was constructed in 1937. One begins with a narrow, collimated, beam of electrons, and directs it at the surface of an object (preferably in vacuum, so that the electrons do not scatter in the air). By reading off the current scattered from the subject, one can build up an image by scanning the beam across the object.

The technique gains significant flexibility from the fact that the scattered electrons contain large amounts of information about the surface on which they impinge. The scattering angle and energy for an electron will depend on the scattering mode, as well as the impact energy. By varying the angle and energies to which the detector is sensitive, as well as the impact energy, a broad array of material properties can be probed.

We will begin our review of this imaging technique with a theoretical exposition of the scattering modes for electrons impinging on a surface, before turning to practical considerations relating to experimental set-up, specimen preparation, and data acquisition and processing. We will conclude with several research applications for SEM.

II. THEORY OF BEAM-SAMPLE INTERACTIONS

The accelerated electrons interact with the nuclei and electrons of the sample material through elastic and inelastic mechanisms, creating reaction products that can then be used for imaging. These include backscattered electrons (BSE), secondary electrons, Auger electrons, and a variety of X-rays.

II.1. Elastic Interactions

Electrons can interact through Coulomb or Rutherford scattering with positively charged target nuclei without loss of energy. The initial energy of the electron beam is elastically converted into Coulomb potential energy with a dependence on the charge of the nucleus. The scattering is therefore cylindrically symmetric about the beam axis and characterized by a dependence on $\sin^{-4}(\theta/2)$, with an interaction probability directly proportional to the Rutherford scattering cross section given by [2]:

$$\frac{d\sigma}{d\Omega} = \left(\frac{zZe^2}{4\pi\epsilon_0}\right)^2 \left(\frac{1}{4T_a}\right)^2 \frac{1}{\sin^4(\theta/2)} \tag{2}$$

Where $\frac{d\sigma}{d\Omega}$ is the differential angular cross-section, Z is the nuclear proton number, T_a is the incident kinetic energy, and the target nucleus is assumed stationary. The distribution of each elastic scattering interaction is forward-directed, but the fraction of incident electrons elastically scattered at large ($> 90°$) angles increases with the sample thickness. Some of these large-angle scattered electrons can escape the sample material in the backward direction as BSE, particularly from scattering off sample atoms on the surface or near-surface layers. These BSE have high energy, from several keV up to elastically scattered BSE with beam energy. Electrons that are backscattered at the surface without penetrating the sample material are removed from the incident beam and prevented from undergoing further interactions in the sample. Electrons that are backscattered at a nonzero depth within the sample can have additional interactions with sample atoms as they exit the surface. Comprehensive analysis of scattering events along electron trajectories can be studied through Monte Carlo codes implemented in simulation software such as CASINO, de-

signed to simulate enough electron trajectories to represent SEM conditions [3]. Figure 1 shows BSE trajectories compared to trajectories of beam electrons fully stopped in the sample by inelastic interactions.

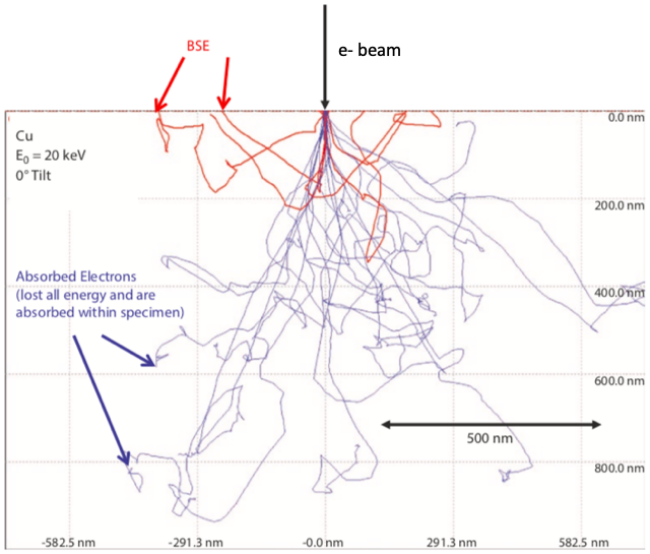

Figure 1. Monte Carlo simulation of a flat, bulk target of copper with 0° tilt for visualization of electron trajectories. Red trajectories lead to backscattering events. (CASINO Monte Carlo simulation) [4]

II.2. Inelastic Scattering

In inelastic interactions, the beam electron energy is not conserved. Some of these inelastic interactions produce detectable signals for use in SEM. Radiative interactions produce a photon, often X-rays. Non-radiative transitions can result in emission of secondary electrons (SE) or Auger electrons [5]. The incident beam electrons can interact with the electrons in atomic electron shells of atoms in the sample material, transferring energy to the atomic electrons. The atomic electrons gain energy and can be excited or even ionized by the interaction, while the beam electrons lose the corresponding amount of energy per interaction. The energy required to displace an atomic electron depends on its electronic shell, and these electrons are labeled with letters according to principle quantum number: K(n=1), L(n=2), M(n=3) and so on [2]. Valence electrons in the atom's outer shells are weakly bound and may become ionized by interaction with the beam electrons. If the ejected electrons have energy greater than the sample material's work function, they can escape the sample surface as SE, with energy of $0-50\,\text{eV}$. Due to inelastic interactions of the low energy SE, the probability of SE escaping and being detected decreases depending how far from the surface the SE was created [6]:

$$p(z) = 0.5 \exp\left(-\frac{z}{\lambda}\right) \tag{3}$$

Where p is the probability, z is the depth from the surface at which the SE was generated, and λ is the mean free path of the SE in the sample material.

Inner or core electrons in the atom's inner shells are more tightly bound. They may become displaced by interaction with beam electrons, leaving a hole in an inner electronic orbital. An outer electron can then transition to the lower energy orbital, emitting a characteristic X-ray corresponding to the electronic shell. If these X-rays exit the sample material, they can be detected and analyzed to provide information on the corresponding atomic orbital transition in the material being studied. If instead of emitting an X-ray, the transition of the outer shell electron to the inner shell hole transfers the corresponding energy to an additional outer shell electron, the outer shell electron can be ionized as an Auger electron. Near the sample surface, these low energy electrons can overcome the work function of the sample and escape towards the detectors. Additional interaction can occur if the X-rays produced by interaction with the electron beam have energies above the sample material electron excitation energies. In this regime, the X-rays produced with electron interaction can fluoresce atoms of the sample material, producing additional, lower energy X-rays. X-rays can be produced by another method: bremsstrahlung or "braking radiation" in which beam electrons are repulsed by the sample electrons and undergo deceleration by emitting a photon that can range in energy from a few eV up to the beam energy [4].

The beam of electrons loses energy at a rate dependent on the density ρ of the sample material:

$$S = -\left(\frac{1}{\rho}\right)\frac{dE_0}{ds}\,, \tag{4}$$

where E_0 is incident beam energy, s is the path length of the beam electron, and S is the rate of energy loss per density [6]. Though Monte Carlo simulations like those shown in Figure 1 are available for detailed descriptions, more practical approximations can be used as an alternative. The energy lost by the electron can be described by a continuous energy loss approximation as proposed by Bethe (1932) [4]:

$$\frac{dE}{ds} = -7.85\left(\frac{Z\rho}{AE_0}\right)\ln\frac{1.166E_0}{J}\ \text{eV/nm}\,, \tag{5}$$

where J is the mean ionization potential in keV. This "Bethe range" gives a description of the penetration of beam electrons into the sample, corresponding to the sample volume that can be analyzed using SEM. Monte Carlo results such as those displayed in Figure 2 can be approximated using the Bethe range if individual trajectories are not required.

The interaction volume directly corresponds to the volume of material that can be studied by the production

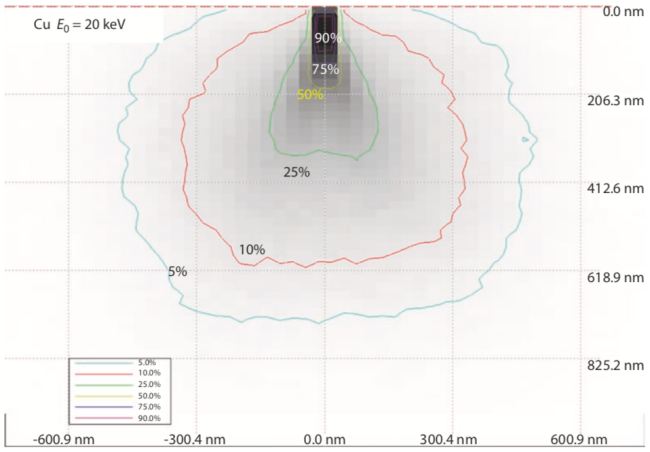

Figure 2. Isocontours of energy loss showing fraction of incident energy remaining; Cu, 20 keV, 0° tilt; 50,000 trajectories (CASINO Monte Carlo simulation) [4]

of detectable signals. Individual beam electrons can undergo a variety of reactions, producing BSE, SE, and X-Rays. SEM equipment is thus designed to detect and process these reaction products in different ways.

III. EXPERIMENTAL SET-UP

An SEM microscope consists of several components divided in three main groups according to their functions: the electron column, responsible for creation and alignment of the electron beam; the specimen chamber, where the electrons interact with the sample and are detected afterwards; and the computer control system, in which image processing is performed and beam scanning is controlled.

III.1. Electron Column

In a vacuum chamber at the beginning of the electron column an electron source generates free electrons, which are subsequently accelerated by a high voltage (typically in the kV range) to produce a beam. The most commonly employed sources are cold field emission guns, tungsten filaments, Schottky field emissions, and LaB_6 emitters. Generally favourable features are high beam stability, high brightness, long lifetime and low beam noise. Which particular type of source will be applicable to a specific set-up depends on the pivotal requirements as these guns show considerable differences in the aforementioned criteria.
The diameter of the electron beam right after emission is up to 50 μm in size. As the achieved spatial resolution depends on the beam diameter (also called probe diameter), focusing to around 10 nm via electromagnetic lenses and apertures is necessary. The former consist of copper coils embedded in a cylindrical iron hull having pole pieces on the inside. Direct current running through these coils

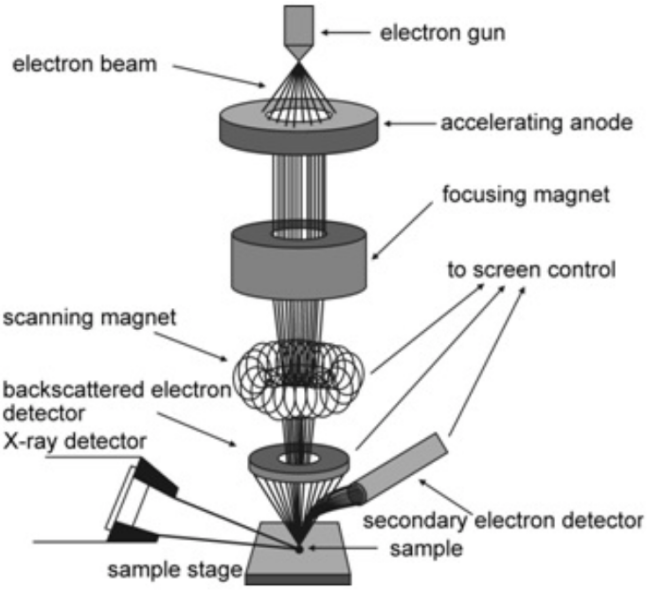

Figure 3. Simple schematic of a standard SEM configuration [7]

produces a magnetic field constricted inside the iron shell except the area of the pole pieces. The electrons of the beam travel through this radially symmetrical field and are focused as depicted in Figure 4. The Lorentz force,

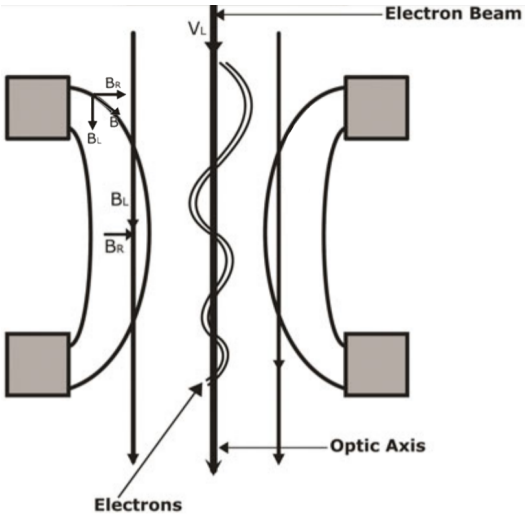

Figure 4. Focusing of the incident electron beam inside the electromagnetic lens. Due to interaction with the magnetic field produced by the pole pieces the electrons are deflected towards the optical axis and the beam diameter decreases [6].

resulting from the radial part of the magnetic field B_R, that is perpendicular to the optical axis of the lens, causes the electrons to circle around the optical axis. Then, the electrons undergo deflection towards the optical axis because of the longitudinal part of the magnetic field B_L. This focusing effect is made particularly effective by the

inhomogeneity of the field, so that at a further distance from the optical axis, a greater force results. The final beam diameter is given by

$$d_0 = \frac{1}{2B}\sqrt{\frac{2mV_0}{e}} \tag{6}$$

where B is the magnetic field strength, m the electron mass, e the electron charge and V_0 the the voltage accelerating the electrons in the electron gun. Depending on the initial beam size, two or three of these condenser lenses are used consecutively before the electrons reach the specimen.

III.2. Specimen Chamber

Inside the specimen chamber detectors are located around the specimen to collect electrons originating from the specimen after interaction. One detector capable of detecting both secondary (SE) and backscattered electrons (BSE), depending on the mode of operation, is the Everhart-Thornley detector. This fist-sized detector is based on a collector-scintillator-photomultiplier interplay and faces the specimen under an angle of around 30 ° in relation to the horizontal (Figure 5).

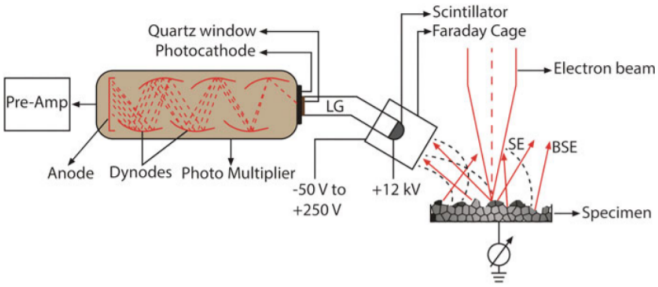

Figure 5. Working principle of an Everhart-Thornley detector. Secondary and backscattered electrons are sucked away by a positive bias and absorbed by a scintillator. The photons emitted by the scintillator in turn are transported out of the vacuum and absorbed by photocathode, where they are detected as a current.[6].

SE emitted by the specimen possess energy of $0-50\,\mathrm{eV}$ and BSE of several keV. By applying a positive potential of 200 V to the grid (Faraday cage) all SE but only line-of-sight and low energy BSE are collected. To convey the information in these electrons beyond the vacuum chamber, they are converted into photons at a scintillator (a material that re-emits the energy of absorbed ionizing radiation in the from of of light). The resulting photons pass out of the vacuum chamber via a quartz window, where they arrive at a photomultiplier tube. There, the photons trigger the ejection of electrons, which are attracted to dynodes (electrode in vacuum) at successively higher voltage. As the electrons hit the dynode, more secondary electrons than incident are emitted, as the incident electrons' energy increases on approach. Eventually, the electron shower so generated is large enough to be detected by the anode as a voltage drop. This voltage drop is passed on to the pre-amplifier for further processing. It is this voltage that corresponds to the the brightness of individual areas in the image. By increasing the potential difference between the dynodes one can increase the contrast of the resulting image as all areas gain signal strength by a certain factor. Changes in the overall brightness are taken via pre-amplification.

By applying a negative potential of about −50V to the Faraday cage instead of a positive one, the SE are rejected, because of their low energy, and only high energetic line-of-sight BSE are detected. This allows the primarily SE detector to detect BSE but rather inefficiently as the majority of BSE possess a high energy and are ejected upward along the beam direction after specimen interaction. Therefore another Everhart-Thornley detector in a doughnut shape concentric around the incident electron beam above the specimen is used for increased detection rate of BSE [6].

IV. SAMPLE PREPARATION

One of the reasons why SEM allows convenient and fast imaging of the surface topography is that it requires little or no sample preparation depending on the material investigated. General prerequisites on the sample are e.g. sufficient electrical conductivity so that grounding can prevent electrostatic charging that would deflect the incident electron beam. Non-conductive materials can be coated with a conductive material. In most cases gold is chosen for this due to its high conductivity and small grain size compared to other possible materials. Furthermore the specimen must be stable in vacuum and able to withstand the bombardment by the electrons without undergoing substantial degradation [4].

V. SIGNAL PROCESSING

V.1. Image Formation

In SEM imaging, like many other imaging techniques, the specimen is rastered using a collimated beam of electrons (also called electron probe) emerging from the microscope column. The information about every discrete location on the specimen is encoded in the intensity of the signal of the secondary electrons (SE) and backscattered electrons (BSE). To each pixel on the finished image exists a corresponding picture element on the specimen. The size of those picture elements depends on the magnification during the imaging. If the signal generating area, which is dependent on probe diameter, is smaller than the respective picture element (dependent on magnification) the picture will be sharp. However, if the signal generating area is bigger than the picture element, the image will appear blurry and out of focus because information from neighbouring picture elements will overlap. So, to gain

maximum performance, the spot size should be adjusted depending on the magnification.

V.2. Signal-to-Noise Ratio

When a specimen is scanned several times, the intensity at a discrete location will show a Gaussian distribution around a mean value. The uncertainty of this mean value is called statistical noise and is evaluated to be $\sqrt{n}$ of the intensity (electrons per second) n. It follows that the signal-to-noise ratio (SNR) is $n/\sqrt{n} = \sqrt{n}$.

One can increase the intensity by increasing the probe current, or increasing how long the SEM lingers over a site (i.e. reducing the scan rate). However, for non-conductive specimens, decreasing the scan rate will result in the specimen accruing a net negative charge, a process called "charge up" (cf. Figure 12), which constrains the scan-rate. For conductive specimens, this is not a problem and slow scan-rates are possible, albeit at the expense of imaging time. So in practice the fastest scan rate that gives a smooth image is chosen.

Additionally, a large solid angle of collection for the signal and frame averaging, as well as editing software can improve the quality of the resulting picture.

There are several models available that can be used to determine the noise in SEM pictures to filter it. On top of the statistical noise described above are several more contributors: secondary emission noise, primary beam noise, and noise from the detection systems also corrupt the signal. These noise sources are well treated in standard texts (e.g. [6]), and are beyond the scope of the present review.

V.3. Contrast Formation

In order to distinguish different features in a SEM picture, the difference in intensity of a picture element compared to the background signal, has to be high. In that way, contrast C can be described as

$$C = \frac{S_\mathrm{A} - S_\mathrm{B}}{S_\mathrm{A}}\,, \tag{7}$$

where S_A is the intensity of a picture element A and S_B the signal of the background.

V.4. Spatial Resolution

In a given optical system that is only limited by diffraction Abbe's equation (1) can be used to determine the upper limit for the resolution d of the SEM. Here, n is the refractive index of the medium between specimen and column and α the half angle of the cone of electrons converging on to the specimen in radians. Using the de Broglie wavelength and the kinetic energy of electrons and substituting it into (1), the resolution d becomes a function of accelerating voltage V:

$$d = \frac{0.753}{\alpha\sqrt{V}} \tag{8}$$

For a maximum accelerating voltage of 30 keV and an α of around 0.01, the theoretical limit of resolution is 0.435 nm. However, due to lens errors and aberrations the precision decreases. Using more advanced techniques like beam monochromators (which select for a single beam e^- wavelength) and immersion optics a maximum resolution of 0.5 nm at 30 keV and 0.9 nm at 1keV can be achieved.

V.4.1. Imaging Parameters

Due to the relatively large interaction volume of the beam (cf. Figure 2), the high resolution part of the signal comes from the SE signal (black spot in Figure 2) which is dependent on the spot size. Because of that, the resolution of the SEM can never be better than the diameter of the probe. So, in order to increase the resolution at a given accelerating voltage, the excitation volume can be further decreased by decreasing the distance between the end of the electron column and the focal point, called Working Distance (WD). When the working distance is decreased, the angle of convergence increases which in turn decreases the spot size. A decrease in probe size is always accompanied by a decrease in the number of electrons in the beam. The decrease in beam current I_C can lead to low contrast C: To evaluate this, the Rose criterion can be used:

$$I_\mathrm{C} > \frac{4 \cdot 10^{-12}}{qFC^2} \tag{9}$$

where F is the scan time and q is the detector efficiency and electron yield. A current of several tens of pA is used for high resolution imaging.

V.4.2. Accelerating Voltage

Higher accelerating voltages produce brighter images and smaller probe sizes, which is suitable for high-Z materials, as well as thin film specimens. For bulk samples with lower atomic numbers, a lower accelerating voltage (500 V - 5 kV) is used to reduce low-resolution signals (BSE and multiply-scattered secondary electrons (SE_2)) caused by a large excitation volume in order to maximize the SNR.

During low voltage microscopy, the excitation volume of the SE_2 signal gets comparably small to the SE signal. This localization increases the amount of SE_2 signal that is emitted from the particular picture element that is being probed and thus enhances the spatial resolution.

Consequences are better performance, contrast and better resolution for BSE and SE signal.

Because the SE signal gain is stronger than the loss in brightness, the SNR remains good. However, feature visibility can be affected if acceleration voltage is too low. Apart from that, the amount of chromatic aberration increases in accordance to (10) due to larger energy spread ΔE at low acceleration voltages:

$$d_0 = C_c \alpha \left(\frac{\Delta E}{E_0} \right) \tag{10}$$

where C_c is the chromatic aberration coefficient and E_0 the beam energy. Along with that goes a loss in contrast as the energy spread alters the beam shape and lowers the intensity in the focal point. An example for the impact of chromatic aberration on the image quality is shown in Figure 13 in the appendix.

Due to the low beam energy the electrons are also more easily affected by electromagnetic fields and thus require a shorter working distance.

In general, low acceleration voltages are more suited for soft or fragile specimen and surface imaging while high acceleration voltages produce better resolution, brighter images and are less susceptible to chromatic aberration. Figure 14 in the appendix shows an image taken with of acceleration voltage of 2 keV and 15 keV respectively.

V.5. Depth of Field

A big advantage of SEM compared to other imaging techniques is the large depth of field. Depth of field means that not only the plane of the focal point is in focus but also other planes above and below the focal plane. A high depth of field D_f can be achieved because the convergence angles and the probe diameter are very small. It can also be expressed in terms of the magnification M, the radius R_{ap} of the final aperture and the working distance WD:

$$D_f \approx \frac{\mathrm{WD} \cdot 200\mu\mathrm{m}}{R_{ap} M} \tag{11}$$

The influence of the aperture on the depth of field is shown in Figure 15 in the appendix. A large depth of field is important when observing topography, morphology and surface details of a specimen (for examples see Figure 16 in the appendix). [6]

VI. APPLICATIONS

VI.1. Practical Motivation for SEM

As supported by the theory outlined above, SEM provides a relatively robust and versatile tool from which very highly magnified images can be extracted and analysed. The following will describe how the unique capabilities of SEM can be applied to current research, engineering and manufacturing. As there exists a plethora of SEM applications, a selection will be reviewed here which spans a broad range of fields including materials engineering, nanotechnology, and thin film device manufacturing. Generally, SEM offers an early design stage imaging tool which provides primarily qualitative information.

VI.1.1. Cross Sectional Analysis of Thin Film Devices

Over the past few decades, clean energy production has become a ubiquitous and invaluable research objective. Traditional inorganic photovoltaics have been proposed and studied as a solution in the past, however the cost, manufacturability and versatility of such devices has led to alternative branches of photovoltaic research. Broadly, one such branch of alternatives is organic solar cells. The devices presented in Figure 6 and Figure 7 [8], are such an organic solar cell, fabricated with a colloidal quantum dot active photovoltaic layer. Quantum dots are unique in the area of photovoltaic devices as they provide room temperature manufacturing, flexibility and a tunable photonic band gap due to the quantum size effect.

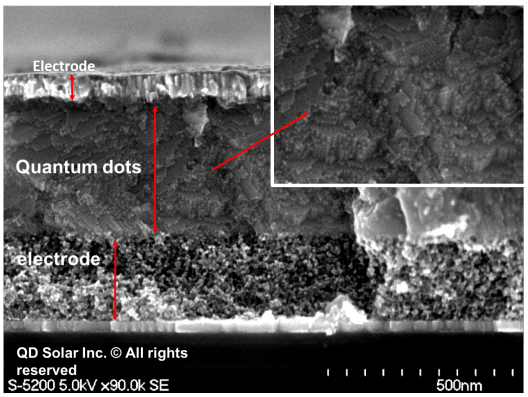

Figure 6. Cross sectional SEM image of a Schottky colloidal quantum dot photovoltaic device. Both electrode layers and the active quantum dot layer are clearly distinguishable. Individual quantum dots are also resolved.

Regardless of the specific composition of a proposed organic photovoltaic device (or any thin film device for that matter), it is essential to be able to visualize and image the cross section of these devices. Although these images would not provide direct quantitative information about the device (other than an approximate film thickness), they provide early design stage insight into the general morphology of the device, and any issues that may be present. As the entire structure is less than a micron thick, and each dot in the CQD layer is on the scale of a nanometer, high magnification and resolution is essential to visualize the device morphology. As depicted

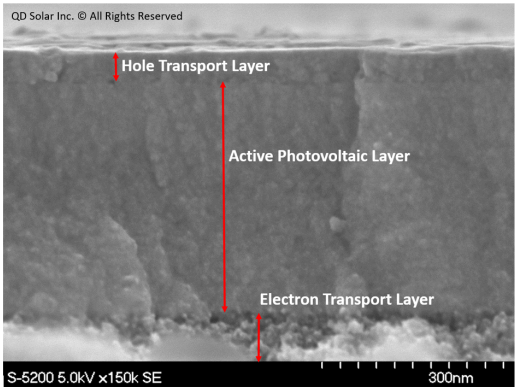

Figure 7. Cross sectional SEM image of a heterojunction colloidal quantum dot photovoltaic device. The line between hole transport and active quantum dot layers can be clearly observed.

in Figure 6, SEM at a magnification of 90 k and 5 kV of power was successful in imaging the full architecture of the device; from electrode to active layer to electrode. Impressively, the SEM was also able to sufficiently resolve each quantum dot within the active layer (which can be seen in the magnified panel in Figure 6). A different device (heterojunction as opposed to Schottky) is displayed in an SEM image in Figure 7, where a distinct line can be observed between two differently sized and treated quantum dot layers (the hole transport layer and the active layer).

VI.1.2. Fractography

Fractography is a primary subset of materials science and engineering, and describes the study of fracture surfaces in materials post mechanical failure. From dental implants, to structural failure, to forensics, fractography persists as an expanding research and engineering field. In terms of SEM usage, especially in the context of recent advances in complex nanomaterials and composite materials, the fracture surface must be magnified and resolved to the nanometer scale for effective diagnoses of a failure mechanism. For example, Figure 8 [9] depicts the failure surface of an alloyed metal hip implant post failure. The striations highlighted in red (somewhere around 500 nm - 1 μm thick) show the crack propagation in the implant moments before fracture, and indicate a fatigue mode of failure. This failure information is paramount to the future design of implants, and it only took one image to determine, demonstrating the value of SEM in a design process.

VI.1.3. Nanostructures

In recent years, nanotechnology and the design of nanomaterials has become a primary research goal in a variety of fields such as materials engineering, medicine,

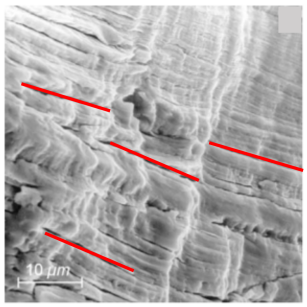

Figure 8. SEM image of CrNiMo-steel hip implant post failure. Red lines indicate striations caused by mechanical fatigue, indicating fatigue failure modes.

and physics due to the novel physical behavior and interactions these materials exhibit. However, to ever properly characterize, fabricate and design with these materials, there must exist an imaging method which can sufficiently resolve their features. With recent advances in SEM performance, this method has become the primary method in imaging and characterizing nanostructures. For example, carbon nanotubes (CNT's) possess unique mechanical, optical/photonic and conductive properties which are being exploited in a variety of current scientific fields. One way of fabricating these structures is to form them within a porous anodic aluminum oxide (AAO) template. Figure 9 [10] depicts an SEM image

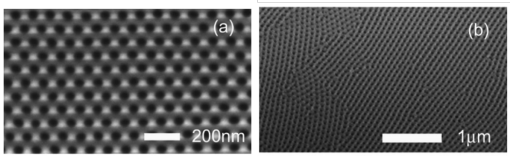

Figure 9. SEM images of porous anodic aluminum oxide template used for growing CNT arrays at a) a high magnification b) a low magnification

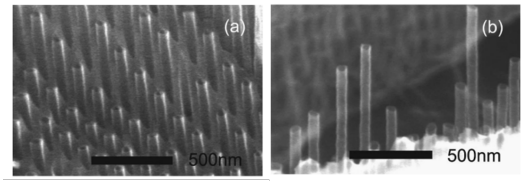

Figure 10. SEM images of the CNT array once the template has been removed, qualitatively confirming a highly ordered, uniform and dense array.

of such a template at different magnifications. This template was used to fabricate the carbon nanotube array shown in Figure 10 [10]. In the case of that study, the goal was to improve the template/fabrication process to produce higher ordered/uniform CNT arrays. After adopting a novel 2 step anodization process, the SEM images of the final product in Figure 10 were used to confirm the proposed hypothesis of increased order, uniformity and

density. This example demonstrates the utility of SEM when designing and characterizing novel nanostructures.

VII. CONCLUSION

SEM provides an invaluable imaging tool in a variety of fields of research and engineering primarily due to the possibility of high magnification and resolution in comparison to other methods. This capability is due to the small wavelength range of the probing electron beam as opposed to the range of an optical microscope. There are a variety of extracted signals including SE, BSE and Auger electrons, which can be used to characterize different features. SEM is relatively simple to operate, can be quickly applied to a wide range of samples, and interpretation of the output images is intuitive. With recent advances in small-scale physics and engineering, SEM has become a routine tool in research and design alike. As SEM technology continuously improves, so does the capability and potential application of the method.

[1] R. P. Feynman, California Institute of Technology, Engineering and Science magazine (1960).
[2] K. Krane, *Introductory Nuclear Physics* (Wiley, 1987).
[3] R. Gauvin, P. Hovongton, and D. Drouin, "Casino: monte carlo simulation of electron trajectory in solids," (2016).
[4] J. I. Goldstein, *Scanning Electron Microscopy and X-Ray Microanalysis* (Springer Science+Business Media LLC, 2018).
[5] R. Mehta, *Interactions, Imaging and Spectra in SEM, Scanning Electron Microscopy, Dr. Viacheslav Kazmiruk (Ed.)* (InTech, 2012).
[6] A. Ul-Hamid, *A Beginners' Guide to Scanning Electron Microscopy* (Springer, 2018).
[7] "High-resolution scanning electron microscopy,".
[8] Unpublished (2018).
[9] M. Moeser (2013).
[10] J. S. Suh and J. S. Lee, Applied Physics Letters **75**, 2047 (1999), https://doi.org/10.1063/1.124911.

Appendix A: Appendix

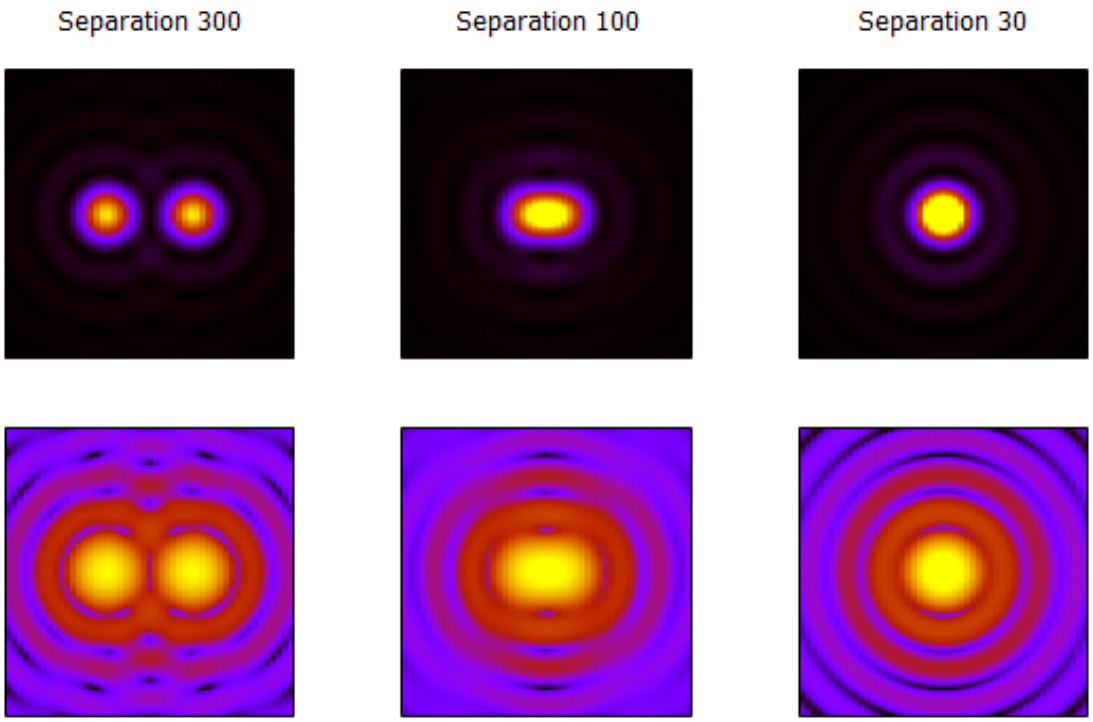

Figure 11. The Airy disks produced from two point sources, as they are moved closer together (in arbitrary units of separation). The bottom row are in log-scale, to improve the visibility of the higher order fringes. [6]

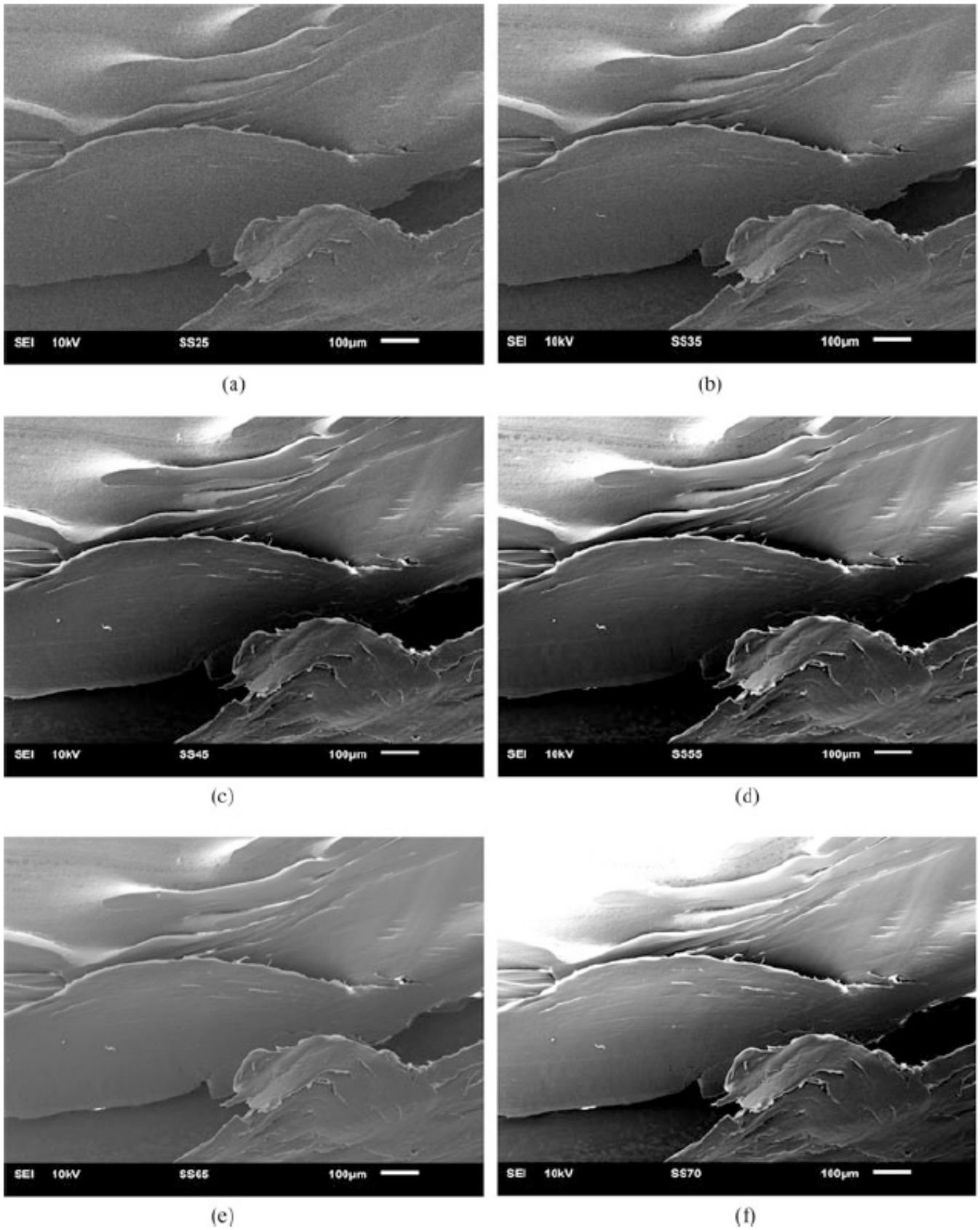

Figure 12. Series of images that show the effect of increasing probe current on a specimen. Probe current increases in each images from (a) to (e). Along with this goes an improvement of SNR and smoothness. (f) Shows the effect of "charge up" in the upper left corner – a saturation in intensity is the consequence. [6]

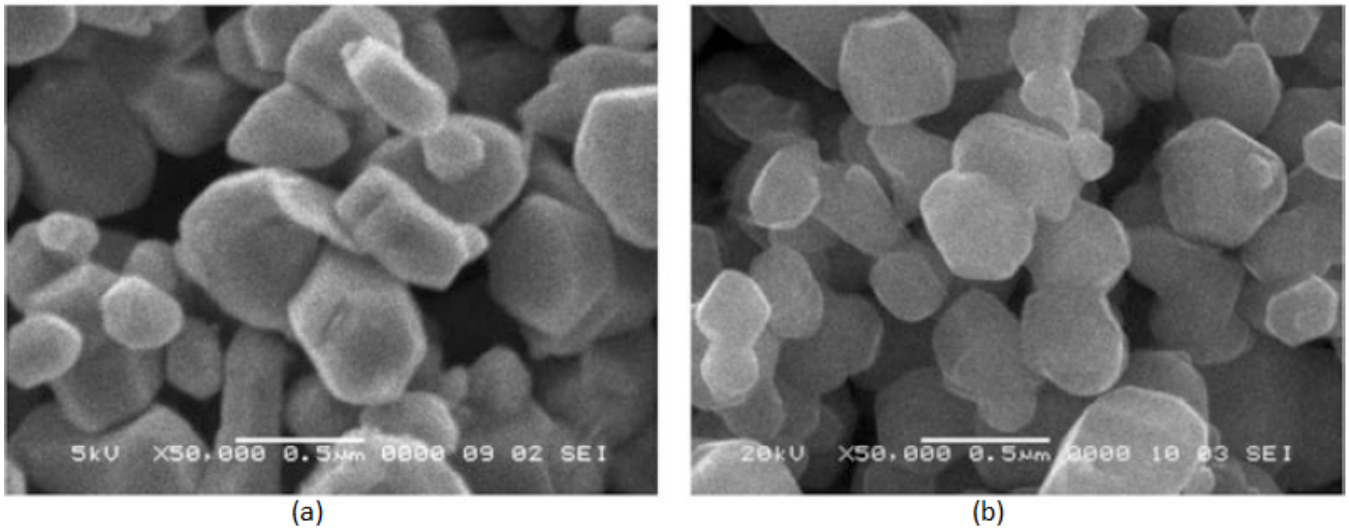

Figure 13. SEM image (a) that shows signs of chromatic aberration at low acceleration voltage of 5 keV which is corrected in (b) with a higher acceleration voltage of 20 keV. In (a) the the contours appear blurred and are sharper in (b).

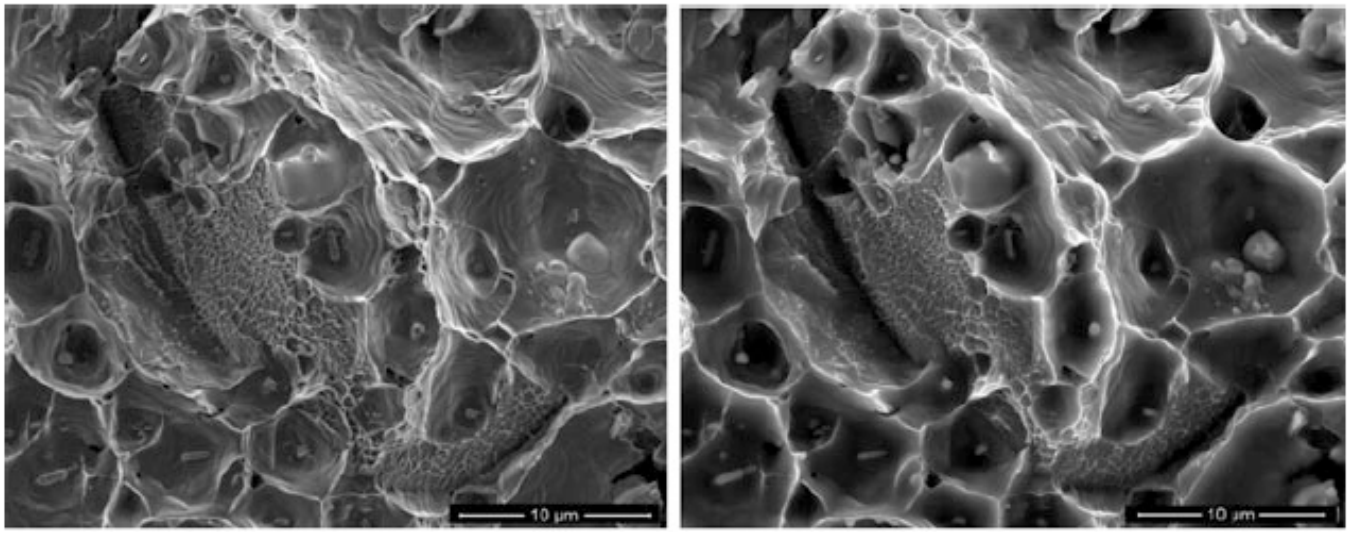

Figure 14. SEM images composed of SE-signals showing the fracture surface of an aluminium specimen. (a) Most structural details are visible at 2 keV acceleration voltage. (b) Surface structure is blurred and features are not clearly discernable, edges are much brighter at 15 keV acceleration voltage [6].

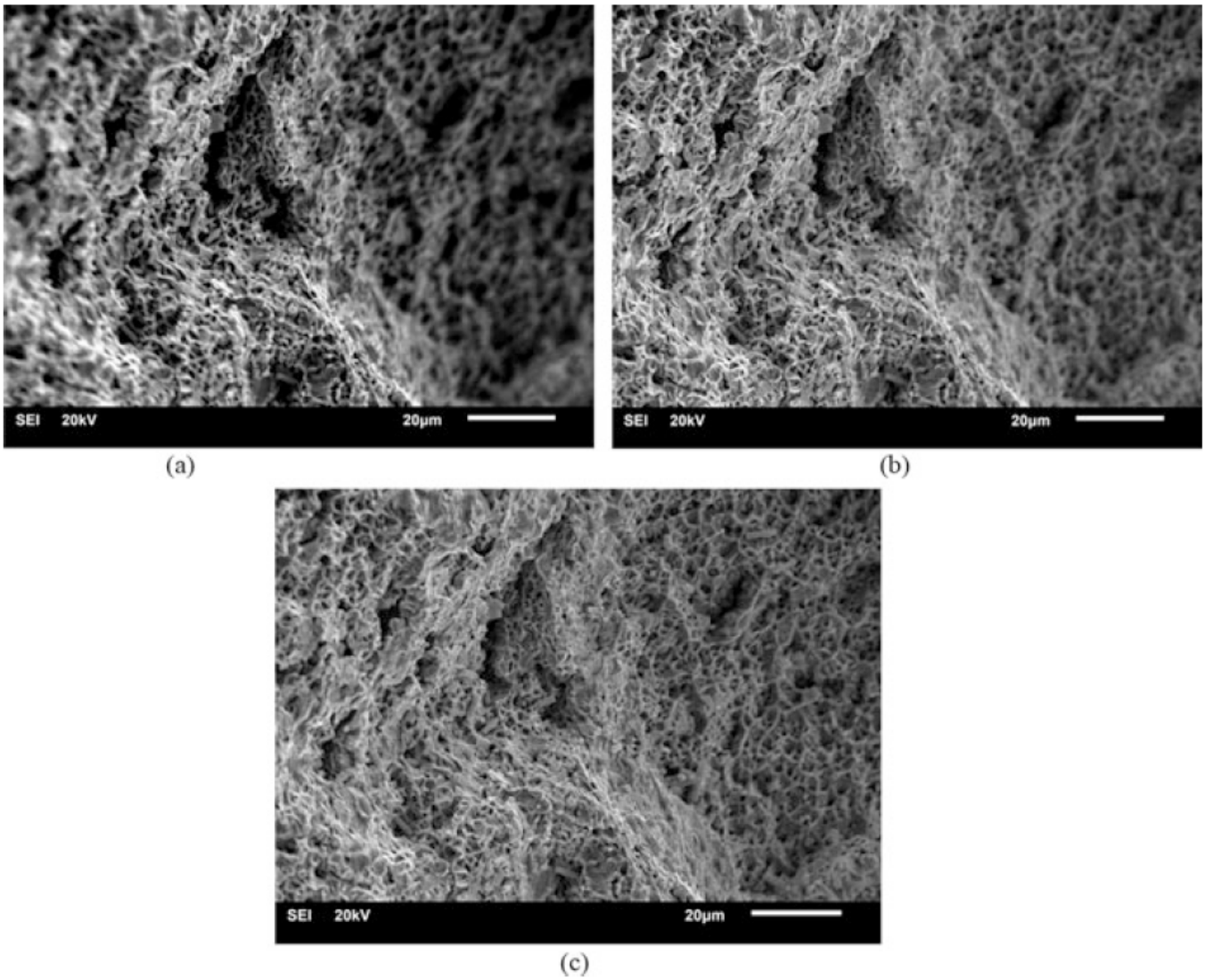

Figure 15. SEM images of a fracture surface at 20 keV acceleration voltage with (a) big, (b) medium and (c) small aperture. As the aperture decreases, more features are in focus [6].

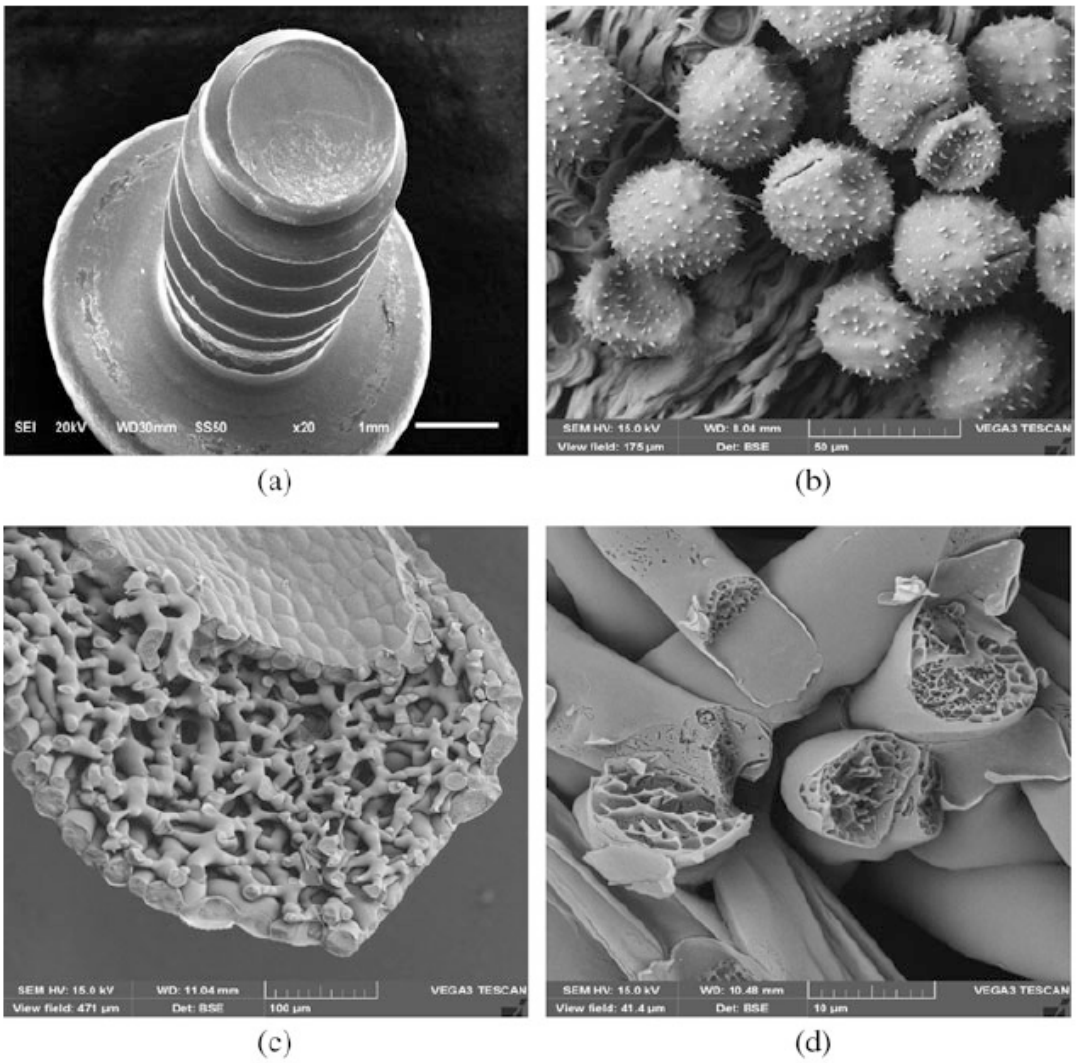

Figure 16. SEM images composed of SE-signals that show the large depth of field. (a) A screw fully in focus from bottom to top. (b-d) Different biological samples [6].